

# **High-density, low temperature ignited operations in FFHR**

**O. Mitarai (Tokai University, Kumamoto Campus)**

**A. Sagara, R.Sakamoto, N. Ohyabu, A. Komori, and O. Motojima (NIFS)**

**Dec. 9-12, 2008**

**18th Toki International Conference (ITC18)**

**Development of Physics and Technology of Stellarator/Heliotrons**

**en route to DEMO (Ceratopia Toki, Gifu, Japan)**

# Contents

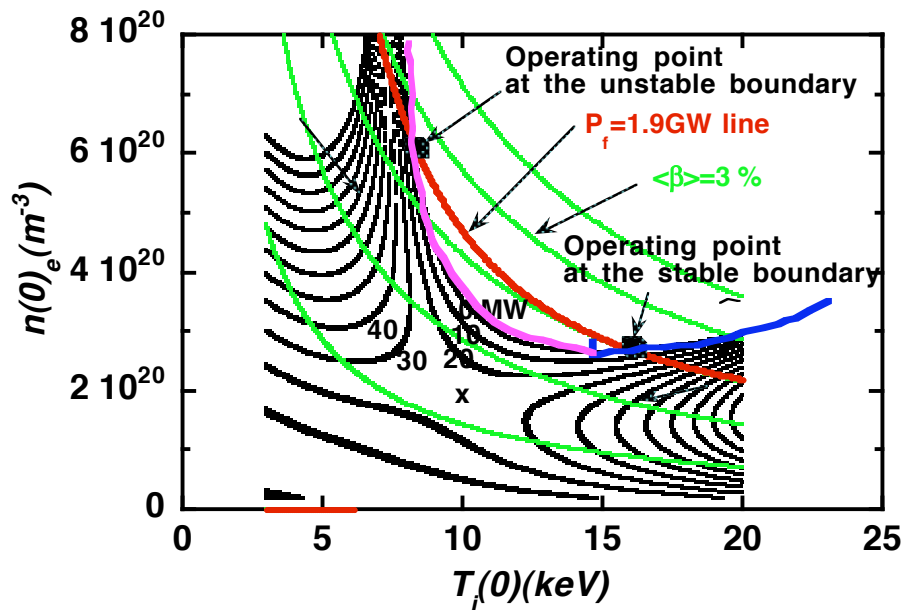
- 1. Motivation of this study**
- 2. 0-D equation and control algorithm**
- 3. Stable to the unstable, and unstable to stable operating point  
(parabolic profiles)**
- 4. Access to the unstable operation point by continuous fueling  
(SDC profile)**
- 5. Access to the unstable operation point by pellet injections.  
(SDC profile)**
- 6. Control robustness to disturbances**
- 7. Shutdown phase**
- 8. Summary and Further issues**

## 1. Motivation of this study:

For the same fusion power, two operating points exist:

- [1] Thermally stable ---- High temperature and low density operation
- [2] Thermally unstable ---- Low temperature and high density operation

Recently, **super-dense core plasma with  $n(0) \sim 1.1 \times 10^{21} \text{ m}^{-3}$**  has been achieved in LHD device with pellet injection experiments. Therefore the low temperature and high-density operation could be a possible operation scenario in FFHR helical reactor.



We need to find how to control the unstable operation in FFHR.

So far many stabilization methods had been proposed in ~40 years.

### **Disadvantages in previous studies:**

- **Linearization is necessary in many equations.**  
Therefore, it is difficult to apply it to 1-D code and a reactor.
- **Only stabilization around the steady state unstable operating point has been shown.**

The access to the unstable operating point from the initial low temperature and density has not been demonstrated.

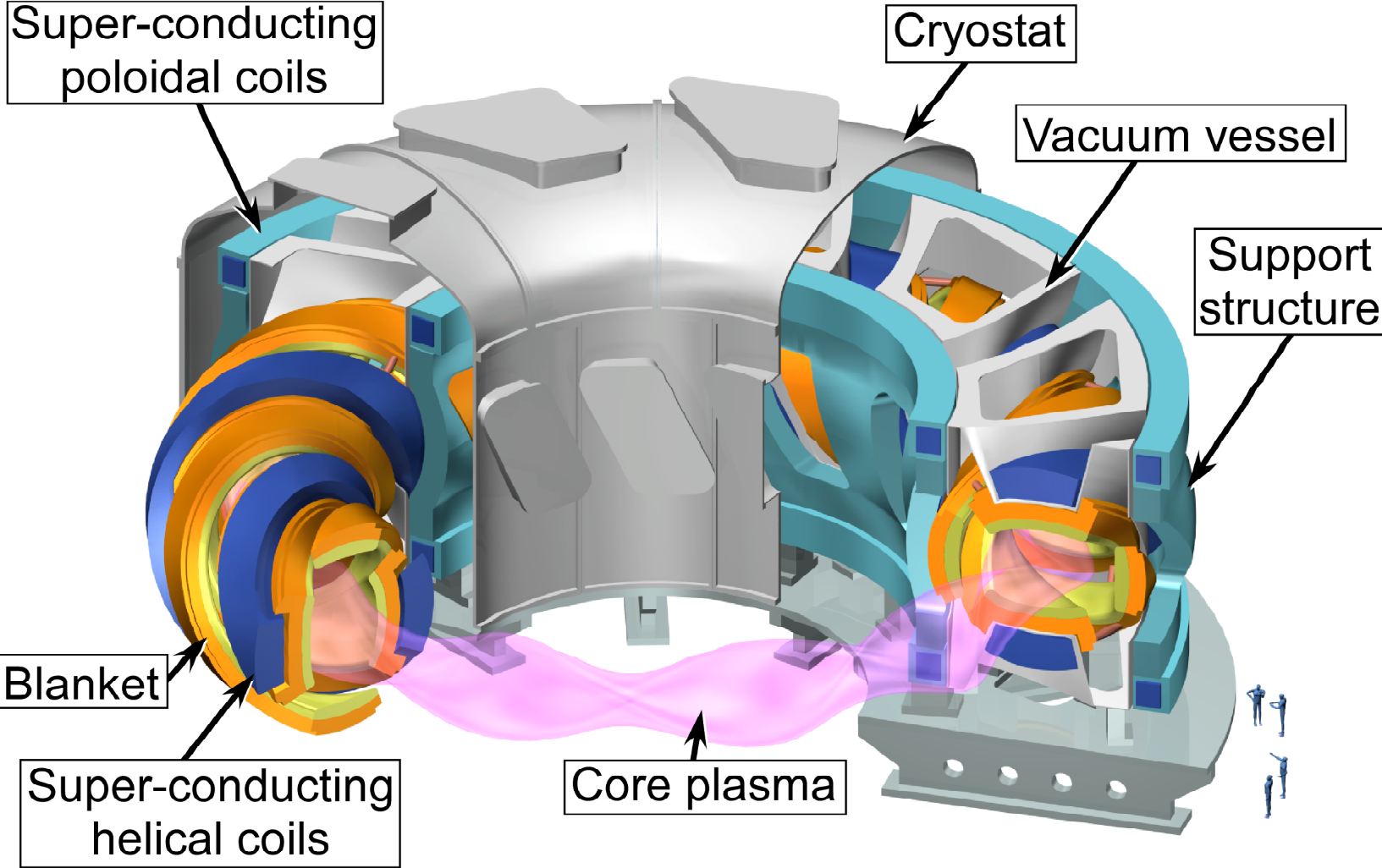
### **Advantages in this control method:**

- **simple PID + comprehensive**
- **no linearization → 0-D and 1-D simulation**
- **Plasma is treated as a black box → possible implementation in a reactor**

## In this study we demonstrate

- **Pellet injection can control the ignition access and steady state operation in the thermally unstable regime using PID fueling control.**
- **Control robustness to various disturbances exists to some extent by pellet injection fueling and heating power.**
- **Smooth fusion power shutdown is possible with pellet injections.**

# FFHR (R=14 m, a=1.72 m, B=6 T)



## 2. 0-D equations and control algorithm

$$\frac{dn_D(0)}{dt} = (1 + \alpha_n)S_D(t) - (1 + \alpha_n)n_D(0)n_T(0)\overline{\langle \sigma V \rangle_{DT}(x)} - \frac{n_D(0)}{\tau_D^*}$$

$$\frac{dn_T(0)}{dt} = (1 + \alpha_n)S_T(t) - (1 + \alpha_n)n_D(0)n_T(0)\overline{\langle \sigma V \rangle_{DT}(x)} - \frac{n_T(0)}{\tau_T^*}$$

$$\frac{dn_\alpha(0)}{dt} = (1 + \alpha_n)n_D(0)n_T(0)\overline{\langle \sigma V \rangle_{DT}(x)} - \frac{n_\alpha(0)}{\tau_\alpha^*}$$

**Charge neutrality condition:**  $n_e(0) = \frac{n_D(0) + n_T(0) + 2n_\alpha(0)}{1 - 8f_o}$

### Combined particle balance equations

$$\frac{dn_e(0)}{dt} = \frac{1}{1 - 8f_o} \left[ (1 + \alpha_n)S_{DT}(t) - \left\{ \frac{f_D + f_T}{\tau_p^*} + \frac{2f_\alpha}{\tau_\alpha^*} \right\} n_e(0) \right]$$

### He ash equations

$$\frac{df_\alpha}{dt} = (1 + \alpha_n)n_e(0)f_D f_T \overline{\langle \sigma V \rangle_{DT}(x)} - \frac{f_\alpha}{\tau_\alpha^*} - \frac{f_\alpha}{n_e(0)} \left[ \frac{dn_e(0)}{dt} \right]$$

## Power balance equation

$$\frac{dT_i(0)}{dt} = \frac{1 + \alpha_n + \alpha_T}{1.5e(f_D + f_T + 1/\gamma_i + f_\alpha)n_e(0)} \times \left[ \{P_{EXT} + P_\alpha\} - \{P_L + P_B + P_S\} \right] - \frac{T_i(0)}{(f_D + f_T + 1/\gamma_i + f_\alpha)} \times \left[ \left\{ 1 - 8f_O + \frac{1}{\gamma_i} - f_\alpha \right\} \frac{1}{n_e(0)} \left[ \frac{dn_e(0)}{dt} \right] - \left[ \frac{df_\alpha(0)}{dt} \right] \right]$$

## 2.2.Profiles

### [1] Thermally stable operation to unstable operation

@Parabolic density profile:  $\alpha_n=1.0$  :  $n(x)/n(0) = (1-x^2)^{\alpha_n}$

@Parabolic temperature profile:

$\alpha_T=1.0$  :  $T(x)/T(0) = (1-x^2)^{\alpha_T}$

### [2] SDC type operation

$\text{Tanh}(x) = (e^x - e^{-x}) / (e^x + e^{-x}) = 1 - 2e^{-x} / (e^x + e^{-x})$

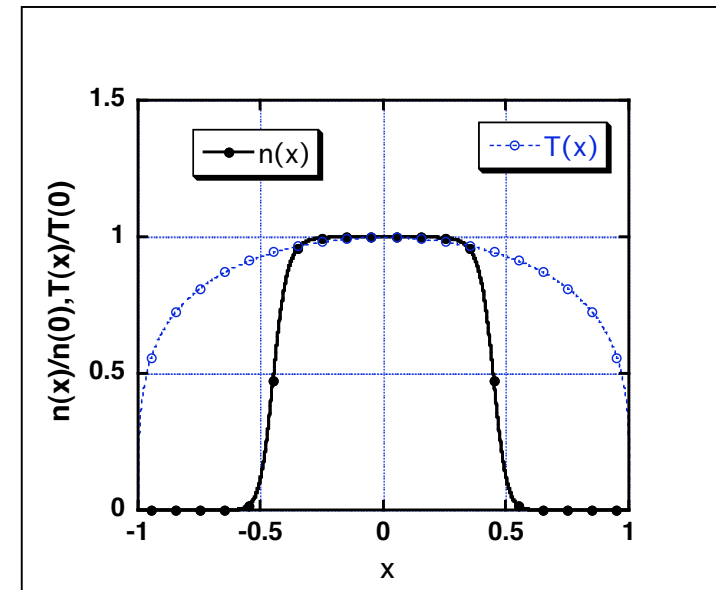
@Box type density profile:

$n(x)/n(0) = 0.5[1 - \text{Tanh}(20(x^2 - a_n))]$

$[\text{row}/a]_{ITBFM} = 0.45$  ( $a_n = 0.2$ )

@Parabolic temperature profile:

$\alpha_T = 0.25$  :  $T(x)/T(0) = (1-x^2)^{\alpha_T}$





## 2.3. Power balance calculation:

**Box type density profile :**

$$n(\rho) = n(0) \times 0.5 \left[ 1 - \text{Tanh} \left\{ 20(\rho^2 - 0.2) \right\} \right]$$

**Parabolic temperature profile:**

$$T(\rho) = T(0)(1 - \rho^2)^{0.25}$$

**@Volume averaged plasma energy:**

$$\begin{aligned} \bar{W} / 3kn(0)T(0) &= \int_0^1 0.5 \left[ 1 - \text{Tanh} \left\{ 20(\rho^2 - 0.2) \right\} \right] \times (1 - \rho^2)^{0.25} 2\rho d\rho \\ &= \frac{1}{1 + \alpha_n + \alpha_T} \Rightarrow 0.194429 \end{aligned}$$

**@Volume averaged Bremsstrahlung loss:**

$$\begin{aligned} \bar{P}_B / \left\{ 1.488 \times 10^{-38} Z_{\text{eff}} n(0)^2 \sqrt{T(0)} \right\} &= \int_0^1 \left\{ 0.5 \left[ 1 - \text{Tanh} \left\{ 20(\rho^2 - 0.2) \right\} \right] \right\}^2 \times (1 - \rho^2)^{0.25/2} 2\rho d\rho \\ &= \frac{1}{1 + 2\alpha_n + 0.5\alpha_T} \Rightarrow 0.172891 \end{aligned}$$

**@Volume averaged alpha heating power :**

**--> direct integration**

## 2.4. ISS95 scaling

$$\begin{cases} \tau_E [s] = \gamma_{ISS} \tau_{ISS95} [s] = \gamma_{LHD} \times 1.6 \tau_{ISS95} [s] \\ \tau_{ISS95} [s] = 0.079 \tau_{2/3}^{0.4} \bar{n}_{19}^{0.51} [10^{19} m^{-3}] B_o^{0.83} [T] \bar{a}^{2.21} [m] R^{0.65} [m] / P_{HT}^{0.59} [MW] \end{cases}$$

## 2.5. Stabilization by PID fueling control

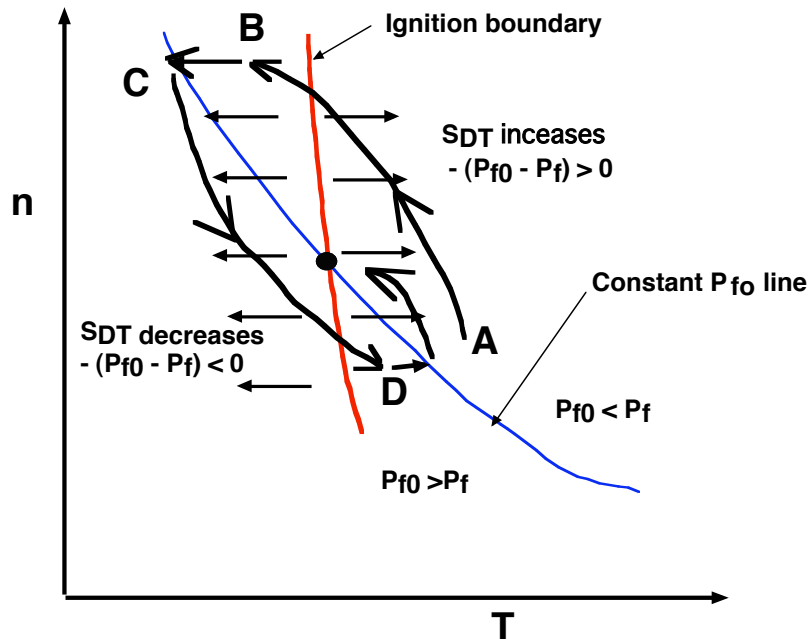
### [1] Continuous fueling

$$S_{DT}(t) = S_{DT0} \left\{ e_{DT}(P_f) + \frac{1}{T_{int}} \int_0^t e_{DT}(P_f) dt + T_d \frac{de_{DT}(P_f)}{dt} \right\} G_{fo}(t) \quad (1)$$

$T_{int}$  the integration time,  $T_d$  the derivative time, [ Note:  $S_{DT}(t)=0$  if  $S_{DT}(t)<0$  ]

The error the fusion power :  $e_{DT}(P_f) = c(1 - P_f/P_{fo})$

- [1]  $c=+1$  for the stable boundary,
- [2]  $c=-1$  for the unstable boundary,



#### @Stabilization mechanism

1. Cooling by fueling and heating by reducing fueling
2. Operation path movement in the sub-and ignition regime

@ During ignition access, a stable control is possible.

## [2] Pellet injection and pellet size

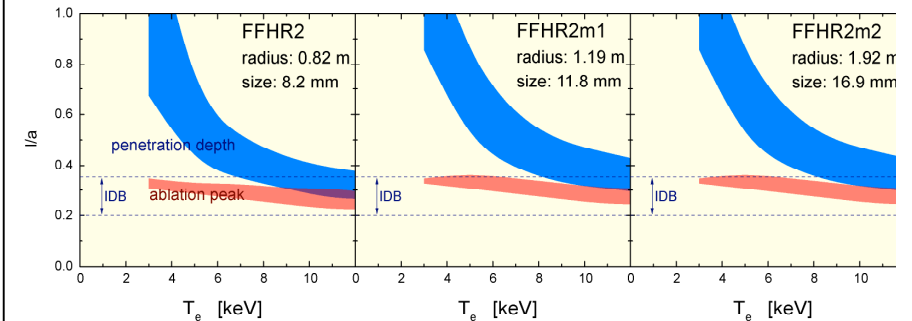
$$Error(P_f) = \left\{ e_{DT}(P_f) + \frac{1}{T_{int}} \int_0^t e_{DT}(P_f) dt + T_d \frac{de_{DT}(P_f)}{dt} \right\}$$

### Discrete fueling

$$\begin{cases} S_{DT}(t) = S_{DT_{pellet}} & \text{for } Error(P_f) > 0 \\ S_{DT}(t) = 0 & \text{for } Error(P_f) \leq 0 \end{cases}$$

Dr. Sakamoto's calculation on the pellet penetration depth in FFHR

~12 mm      ~17 mm



@Plasma Volume  $V_p = 827 \text{ m}^3$       @DT solid molar volumes =  $19.88 \text{ mm}^3/\text{mol}$

@DT ice particle number density =  $\{6.02 \times 10^{23} \times 2\} / 19.88 \text{ [mm}^3/\text{mol}] = 6.05 \times 10^{28} / \text{m}^3$

[1] **L=12mm:**  $N_{pell} = \left\{ \pi \left( L_p / 2 \right)^2 L_p \right\} \times 6.05 \times 10^{28} = 82 \times 10^{21} / \text{m}^3$

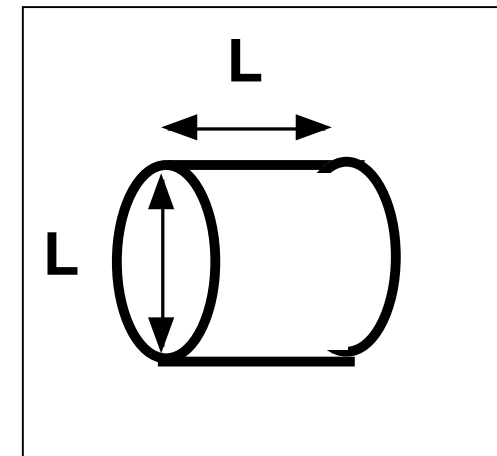
$$\rightarrow S_{DT_{pell}} = N_{pell} / V_p = 0.990 \times 10^{20} / \text{m}^3$$

[2] **L=14mm:**  $N_{pell} = 130 \times 10^{21} / \text{m}^3$

$$\rightarrow S_{DT_{pell}} = N_{pell} / V_p = 1.57 \times 10^{20} / \text{m}^3$$

[3] **L=16mm:**

$$N_{pell} = 194 \times 10^{21} / \text{m}^3 \rightarrow S_{DT_{pell}} = N_{pell} / V_p = 2.353 \times 10^{20} / \text{m}^3$$



## 2.6. Heating power:

In the stable ignition regime, **the density limit scaling** can be used for the feedback control **from ignition to sub-ignition**.

$$\gamma_{DLM} n(0) \leq n(0)_{\text{lim}} [m^{-3}] = \gamma_{SUDO} \frac{0.25 \times 10^{20}}{\gamma_{pr}} \sqrt{\frac{\{P_{NET} [W] \times 10^{-6}\} B_o [T]}{\bar{a}^2 R [m]}}$$

as

$$P_{EXT} [W] = \left\{ \gamma_{pr} \frac{[\gamma_{DLM} n(0) [m^{-3}]]}{\gamma_{SUDO} 0.25 \times 10^{20}} \right\}^2 \frac{\bar{a}^2 R [m]}{B_o [T]} \times 10^6 - (P_\alpha - P_B - P_S)$$

In the unstable ignition regime: this cannot be used.

**[1] Preprogram is used so far.**

**[2] PI control of the heating power is newly developed.**

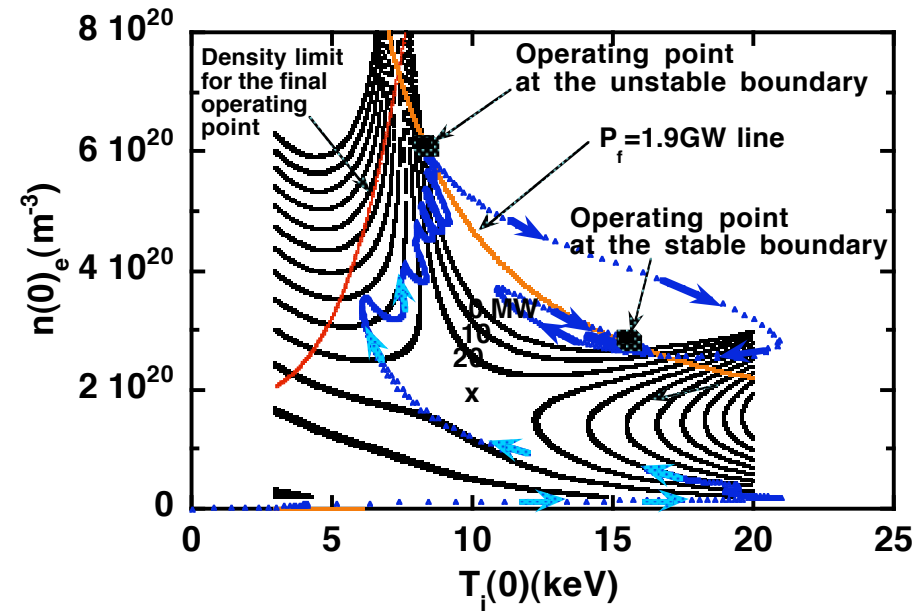
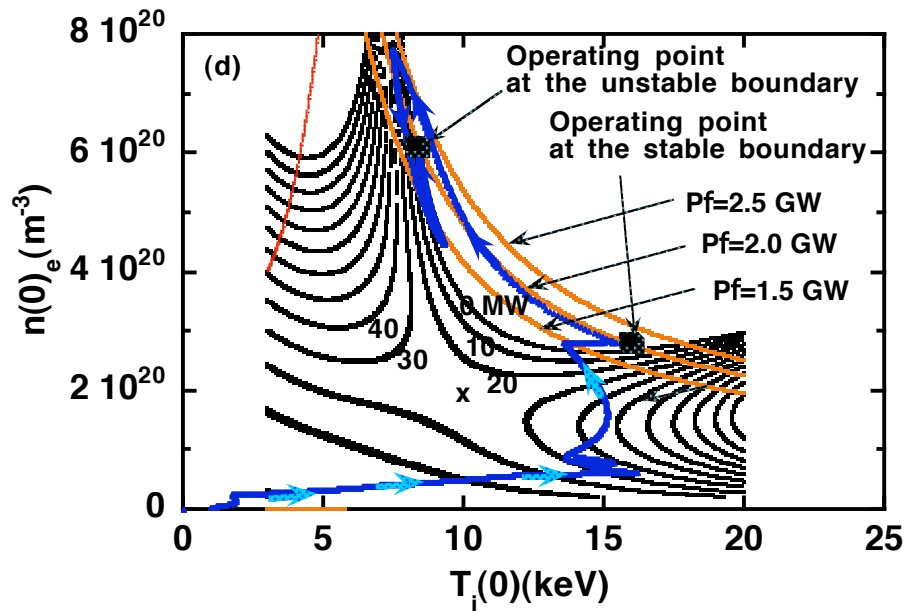
$$P_{EXT} (P_f) = P_{EXTO} \left\{ e_{EXT} (P_f) + \frac{1}{T_{P_{int}}} \int_0^t e_{EXT} (P_f) dt \right\}$$

where  $e_{EXT}(P_f) = (1 - P_f / P_{fimp})$      $P_{fimp}(t) = P_{fo}(t)(1.8/1.9)$ ,     $T_{pint} = 15$  s

### 3. Stable to the unstable, and unstable to stable operating point (parabolic profile, continuous fueling)

**stable to unstable**

**unstable to stable**



Confinement time :

$\tau_E \sim 1.92 \text{ s}$

Divertor heat flux(10cm with) :

$\Gamma_{div} \sim 16 \text{ MW/m}^2$

Bremsstrahlung loss power :

$P_B \sim 57 \text{ MW}$

Beta value :

$\langle \beta \rangle \sim 3.0 \%$

**Unstable point**

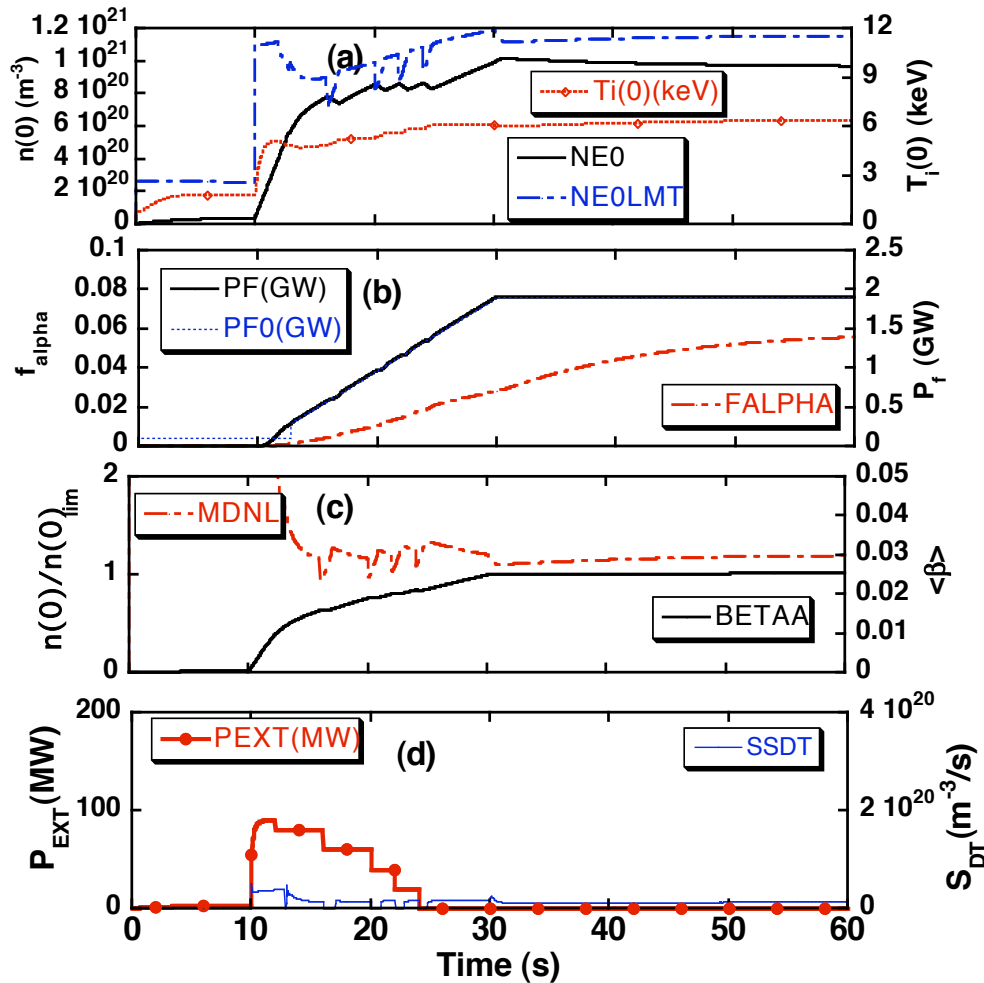
$\tau_E \sim 3.9 \text{ s}$

$\Gamma_{div} \sim 9.1 \text{ MW/m}^2$

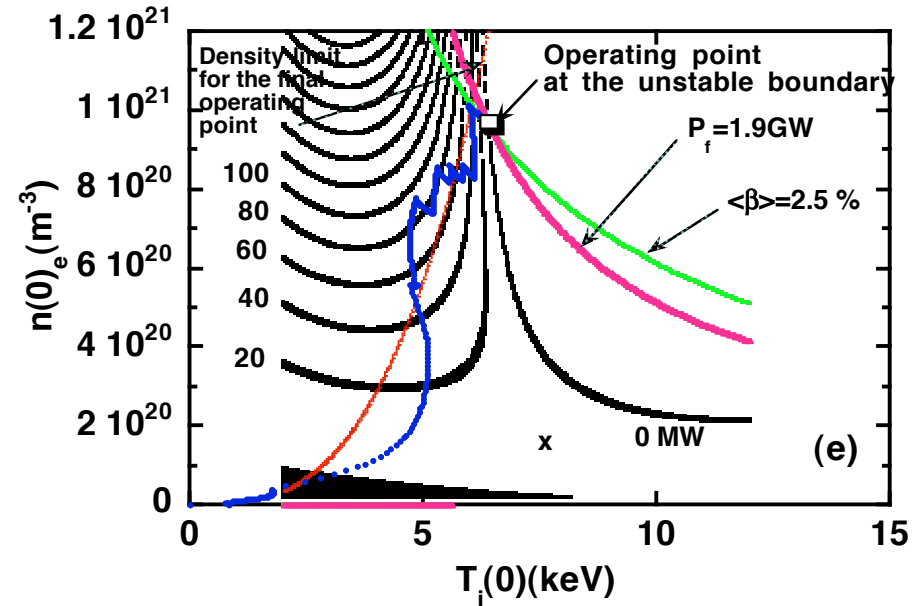
$P_B \sim 181 \text{ MW}$

$\langle \beta \rangle \sim 3.6 \%$

# 4. Access to the unstable operation point by continuous fueling (SDC profile)



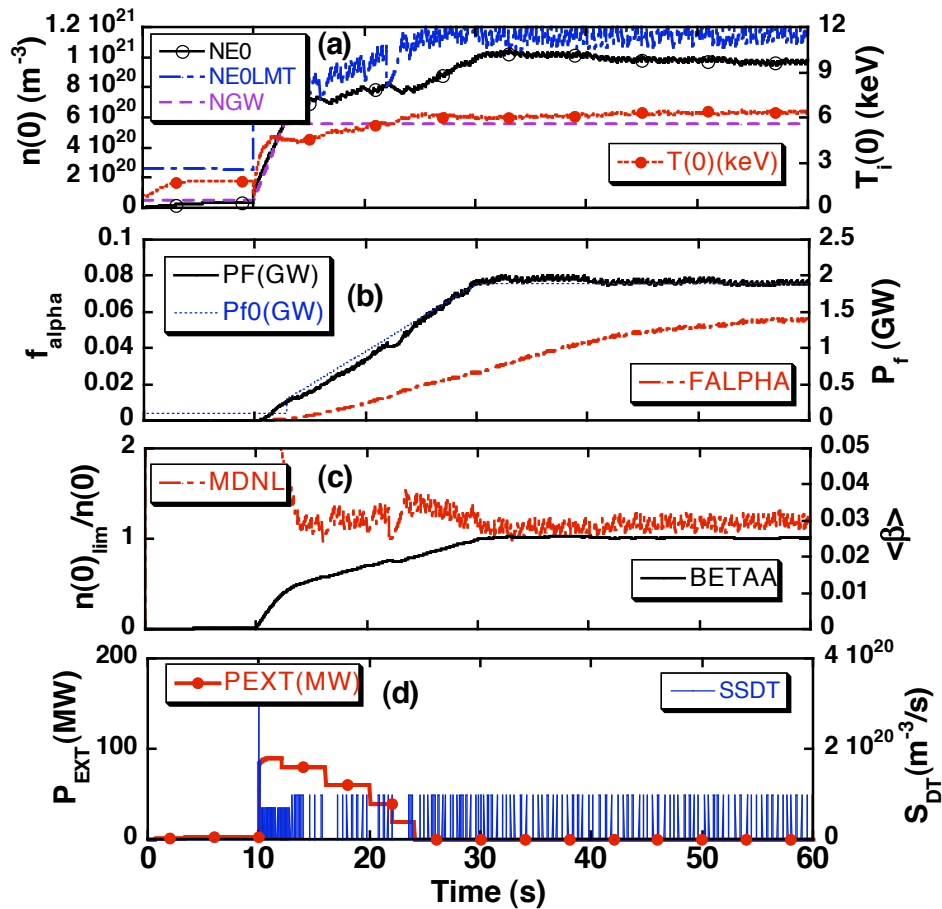
Smooth density and temperature variations by continuous fueling. **This is the basic operation waveform for the following pellet injection.**



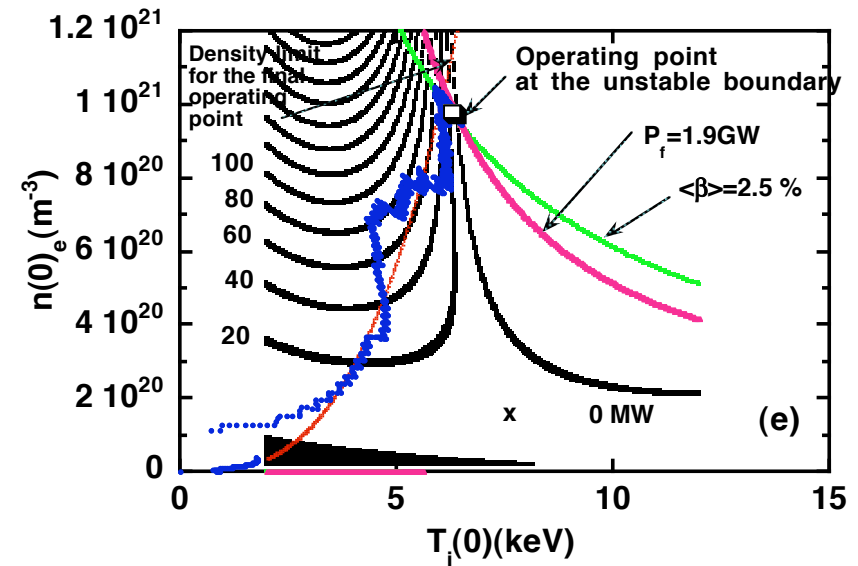
# 5. Access to the unstable operation point by pellet injections.

## [1] 12 mm pellet size

It is possible to control the unstable operating point for  $\Delta n \sim 2.5 \times 10^{19} \text{ m}^{-3}$ .



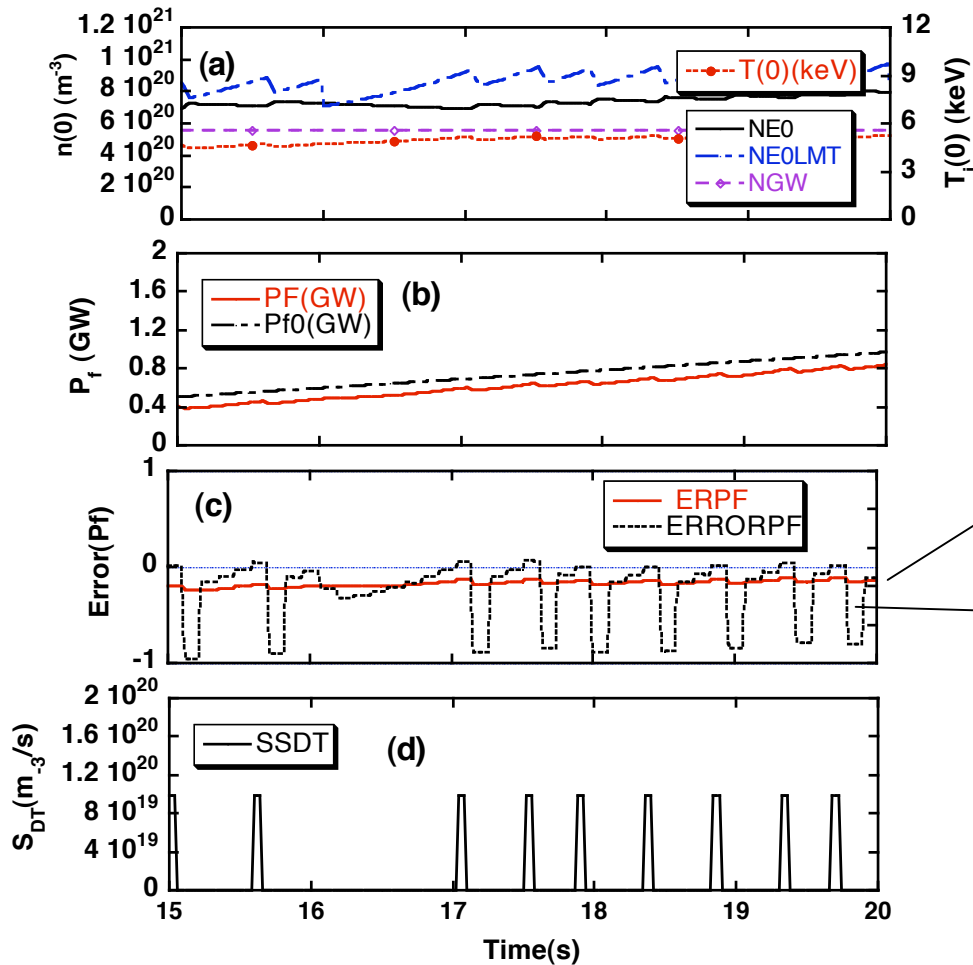
$n(0) = 9.62 \times 10^{20} \text{ m}^{-3}$ ,  $T_i(0) = 6.4 \text{ keV}$ ,  
 $f_{\alpha} = 5.84 \%$ ,  $\langle \beta \rangle = 2.5 \%$



POPCON

During the fusion power rise-up phase, **careful adjustment of  $T_d$  is necessary**, compared to continuous fueling.

( $T_d=0.26s, T_{int}=8s$ )



During the fusion power rise-up phase,  $P_f < P_{f0}$  holds and no fueling by P-control alone.

--> **Derivative time  $T_d$  is important**

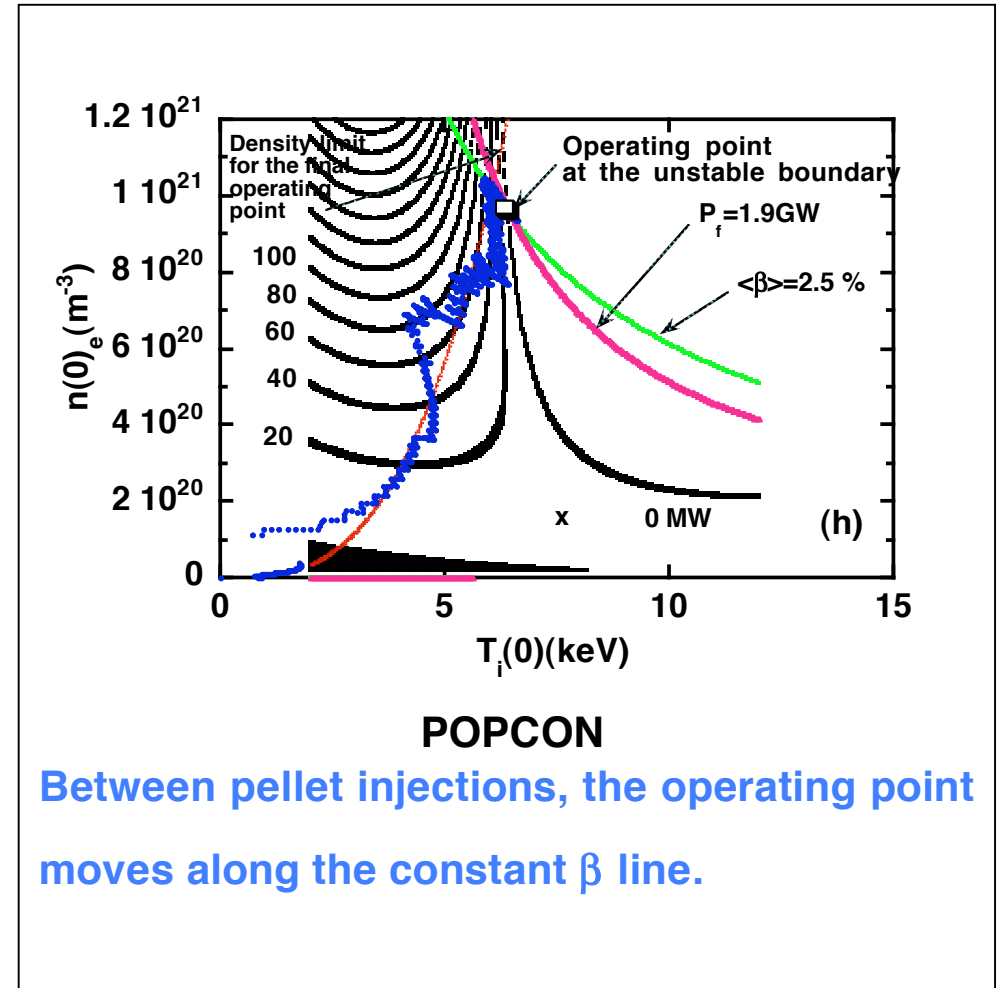
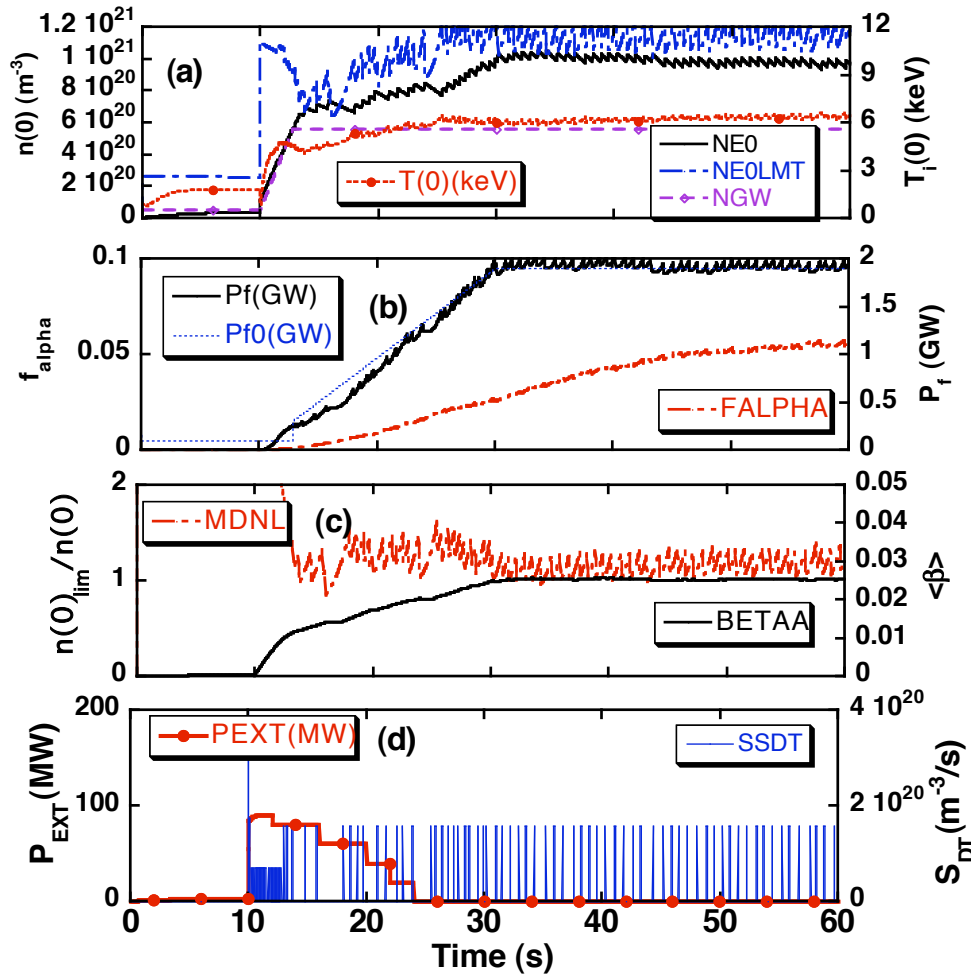
$$ERPF = \{e_{DT}(P_f)\}$$

$$ERRORPF = \left\{ e_{DT}(P_f) + \frac{1}{T_{int}} \int_0^t e_{DT}(P_f) dt + T_d \frac{de_{DT}(P_f)}{dt} \right\}$$



## [2] 14 mm pellet size ( $T_d=0.26s, T_{int}=8s$ )

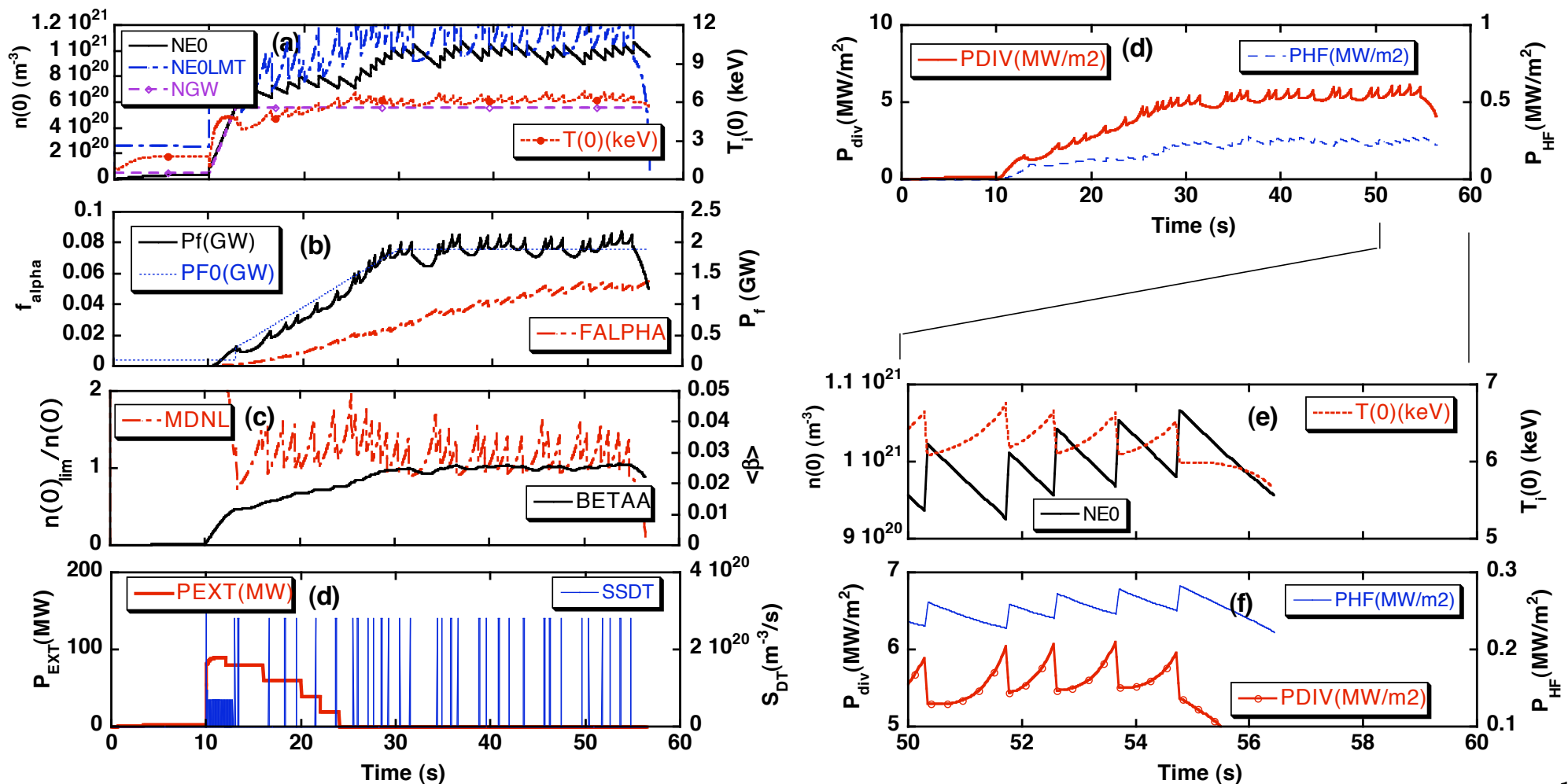
It is still possible to control the unstable operating point for  $\Delta n \sim 5.0 \times 10^{19} \text{ m}^{-3}$ .



**[3] 17 mm pellet size** ( $T_d=0.26s, T_{int}=8s$ )

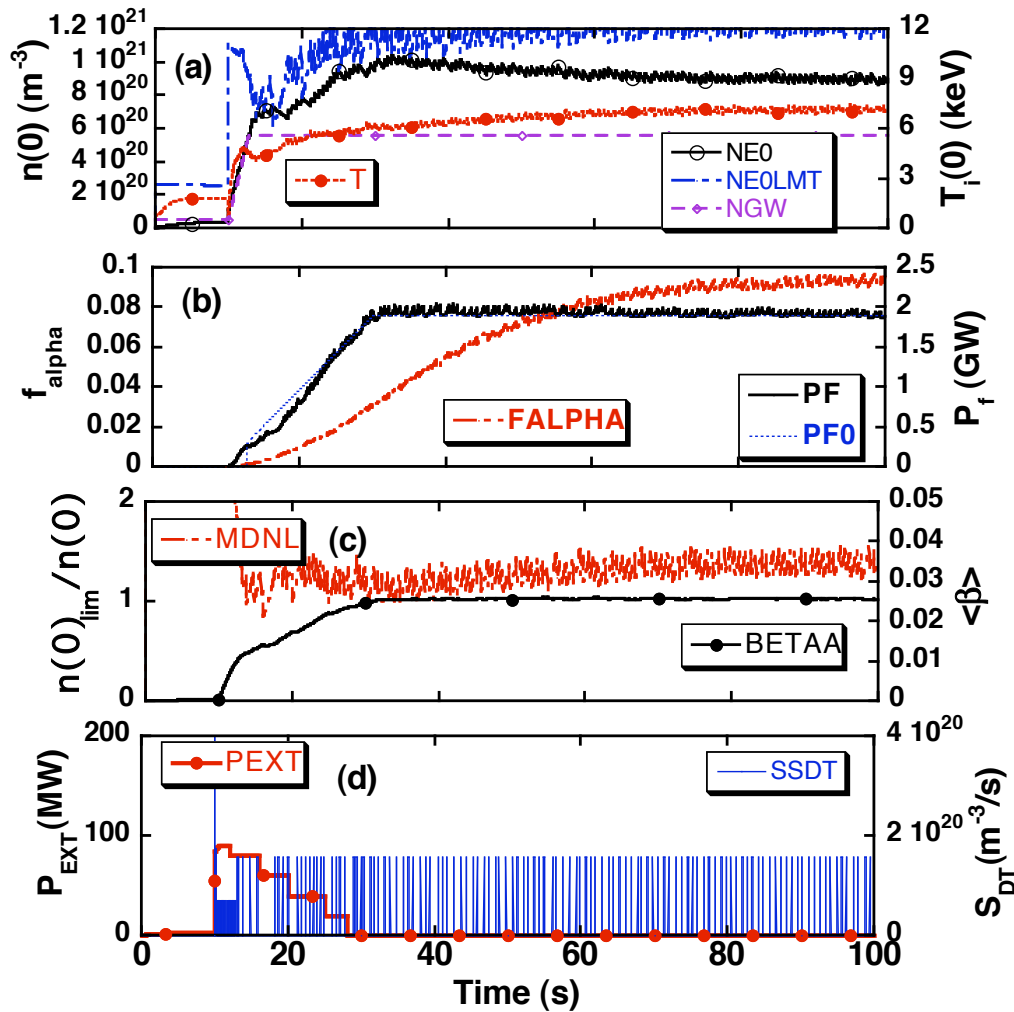
**@ Ignition is terminated due to large variation of temperature and density  $\Delta n \sim 8 \times 10^{19} m^{-3}$ .**

**@ The density and temperature variation are in phase at termination.**



### 5.3. Larger alpha ash confinement time ratio: $\tau_{\alpha}^*/\tau_E=5$ , $\tau_p^*/\tau_E=3$ , $\gamma_{ISS}=1.6$

( $T_d=0.26s, T_{int}=8s$ ) The density is lower and temperature is higher.



14mm pellet,

$n(0)=8.9 \times 10^{20} m^{-3}$ ,

$T_i(0)=7.1$  keV,

$f_{\alpha}=8.9$  %,

$\langle\beta\rangle=2.55$  %

$\Gamma_{div}=6.3$  MW/ $m^2$ ,

$Z_{eff}=1.60$ ,

## Comparison of the plasma parameters at the stable and unstable operating point

|   |  | Steady state value     |                          |             |
|---|--|------------------------|--------------------------|-------------|
|   |  | Stable operating point | Unstable operating point |             |
|   |  | Parabolic profile      | Parabolic profile        | SDC profile |
| Major radius                                    | R (m)  | 14.0                   |                          |             |
| Effective minor radius                          | $\bar{a}$ (m)  | 1.73                   |                          |             |
| Coil pitch parameter                            | $\gamma$   | 1.15                   |                          |             |
| Magnetic field                                  | B <sub>0</sub> (T)                                       | 6.0                    |                          |             |
| <b>Confinement factor over ISS95 scaling</b>    | $\gamma_{ISS}$   | <b>1.92</b>            |                          | <b>1.6</b>  |
| <b>Confinement time</b>                         | $\tau_E$ (s)   | <b>1.9</b>             | <b>3.9</b>               | <b>4.7</b>  |
| Helium ash fraction                             | f <sub>α</sub>   | 0.034                  | 0.034                    | 0.058       |
| Oxygen impurity fraction                        | f <sub>o</sub>   | 0.0075                 |                          |             |
| Effective ion charge                            | Z <sub>eff</sub>   | 1.48                   |                          |             |
| He ash confinement time ratio                   | $\tau_{\alpha}^*/\tau_E$                                 | 3                      |                          |             |
| Fuel particle confinement time ratio            | $\tau_p^*/\tau_E$  | 3                      |                          |             |
| <b>Operation density</b>                        | <b>n<sub>e</sub>(0) (10<sup>20</sup> m<sup>-3</sup>)</b> | <b>2.8</b>             | <b>6.0</b>               | <b>9.6</b>  |
| Density limit factor over Sudo scaling          | $\gamma_{SUDO}$  | 1.5                    | 4.5                      | 5.5         |
| Density limit margin in the steady state        | [n(0) <sub>limit</sub> /n(0)]                            | 1.27                   | 1.36                     | 1.59        |
| <b>Ion temperature</b>                          | <b>T<sub>i</sub>(0) (keV)</b>                            | <b>15.3</b>            | <b>8.5</b>               | <b>6.4</b>  |
| Density profile                                 | $\alpha_n$   | 1.0                    |                          | Box type    |
| Temperature profile                             | $\alpha_T$   | 1.0                    |                          | 0.25        |
| <b>Beta value</b>                               | <b>&lt;β&gt;(%)</b>                                      | <b>3.0</b>             | <b>3.6</b>               | <b>2.5</b>  |
| Plasma energy                                   | W <sub>p</sub> (MJ)                                      | 547                    | 634                      | 448         |
| Fusion power                                    | P <sub>f</sub> (MW)                                      | 1900                   |                          |             |
| Neutron power                                   | P <sub>n</sub> (MW)                                      | 1520                   |                          |             |
| Alpha heating power                             | P <sub>α</sub> (MW)                                      | 380x0.9                |                          |             |
| <b>Bremsstrahlung power</b>                     | <b>P<sub>B</sub>(MW)</b>                                 | <b>57</b>              | <b>181</b>               | <b>248</b>  |
| Synchrotron radiation power                     | P <sub>S</sub> (MW)                                      | 3.4                    | 0.97                     | 0           |
| <b>Plasma conduction loss</b>                   | <b>P<sub>L</sub>(MW)</b>                                 | <b>282</b>             | <b>160</b>               | <b>96</b>   |
| Neutron wall loading                            | Γ <sub>n</sub> (MW/m <sup>2</sup> )                      | 1.5                    |                          |             |
| Heat flux to first wall                         | Γ <sub>h</sub> (MW/m <sup>2</sup> )                      | 0.06                   | 0.18                     | 0.25        |
| <b>Heat flux to divertor for 0.1m wet width</b> | <b>Γ<sub>div</sub>(MW/m<sup>2</sup>)</b>                 | <b>16</b>              | <b>9.1</b>               | <b>5.4</b>  |

## 5.4. Relationship between the energy confinement time, He ash confinement time ratio, and operating temperature and density

| $\gamma_{ISS}$ | $\tau_{\alpha}^*/\tau_E$ | $n(0)$                               | $T(0)$   | $Z_{eff}$ | $f_{\alpha}$ | $P_{div}$              | $\langle\beta\rangle$ |
|----------------|--------------------------|--------------------------------------|----------|-----------|--------------|------------------------|-----------------------|
| 1.2            | 3.0                      | $6.77 \times 10^{20} \text{ m}^{-3}$ | 7.77 keV | 1.48      | 3.28         | 12.1 MW/m <sup>2</sup> | 2.18                  |
|                | 3.5                      | 6.43                                 | 8.12     | 1.49      | 3.83         | 12.6                   | 2.16                  |
| 1.3            | 3.0                      | 8.19                                 | 6.89     | 1.49      | 3.79         | 9.29                   | 2.33                  |
|                | 4.0                      | 7.84                                 | 7.22     | 1.52      | 5.01         | 9.75                   | 2.32                  |
|                | 5.0                      | 7.45                                 | 7.62     | 1.54      | 6.22         | 10.3                   | 2.32                  |
|                | 6.0                      | 6.98                                 | 8.15     | 1.56      | 7.40         | 11.1                   | 2.30                  |
|                | 6.5                      | 6.67                                 | 8.51     | 1.57      | 7.99         | 11.5                   | 2.29                  |
| 1.4            | 3.0                      | 8.89                                 | 6.59     | 1.50      | 4.40         | 7.63                   | 2.41                  |
|                | 4.0                      | 8.57                                 | 6.90     | 1.53      | 5.80         | 8.01                   | 2.42                  |
|                | 5.0                      | 8.23                                 | 7.24     | 1.56      | 7.17         | 8.44                   | 2.43                  |
|                | 6.0                      | 7.86                                 | 7.65     | 1.59      | 8.49         | 8.96                   | 2.42                  |
|                | 7.0                      | 7.44                                 | 8.14     | 1.61      | 9.78         | 9.61                   | 2.42                  |
|                | 7.5                      | 7.19                                 | 8.44     | 1.62      | 10.41        | 10.0                   | 2.42                  |
| 1.5            | 3.0                      | 9.33                                 | 6.46     | 1.52      | 5.09         | 6.45                   | 2.48                  |
|                | 4.0                      | 9.01                                 | 6.78     | 1.55      | 6.69         | 6.79                   | 2.48                  |
|                | 5.0                      | 8.66                                 | 7.13     | 1.58      | 8.24         | 7.19                   | 2.49                  |
|                | 6.0                      | 8.30                                 | 7.53     | 1.61      | 9.73         | 7.67                   | 2.50                  |
|                | 7.0                      | 7.91                                 | 8.01     | 1.64      | 11.1         | 8.23                   | 2.51                  |
|                | 7.5                      | 7.70                                 | 8.27     | 1.65      | 11.8         | 8.56                   | 2.52                  |
| 1.6            | 3.0                      | 9.62                                 | 6.41     | 1.53      | 5.84         | 5.55                   | 2.52                  |
|                | 4.0                      | 9.27                                 | 6.75     | 1.57      | 7.65         | 5.89                   | 2.53                  |
|                | 5.0                      | 8.91                                 | 7.14     | 1.60      | 9.39         | 6.28                   | 2.55                  |
|                | 6.0                      | 8.54                                 | 7.57     | 1.64      | 11.04        | 6.74                   | 2.57                  |
|                | 7.0                      | 8.15                                 | 8.07     | 1.67      | 12.59        | 7.29                   | 2.59                  |
|                | 7.5                      | 7.94                                 | 8.35     | 1.68      | 13.32        | 7.60                   | 2.63                  |

$$[\tau_p^*/\tau_E=3]$$

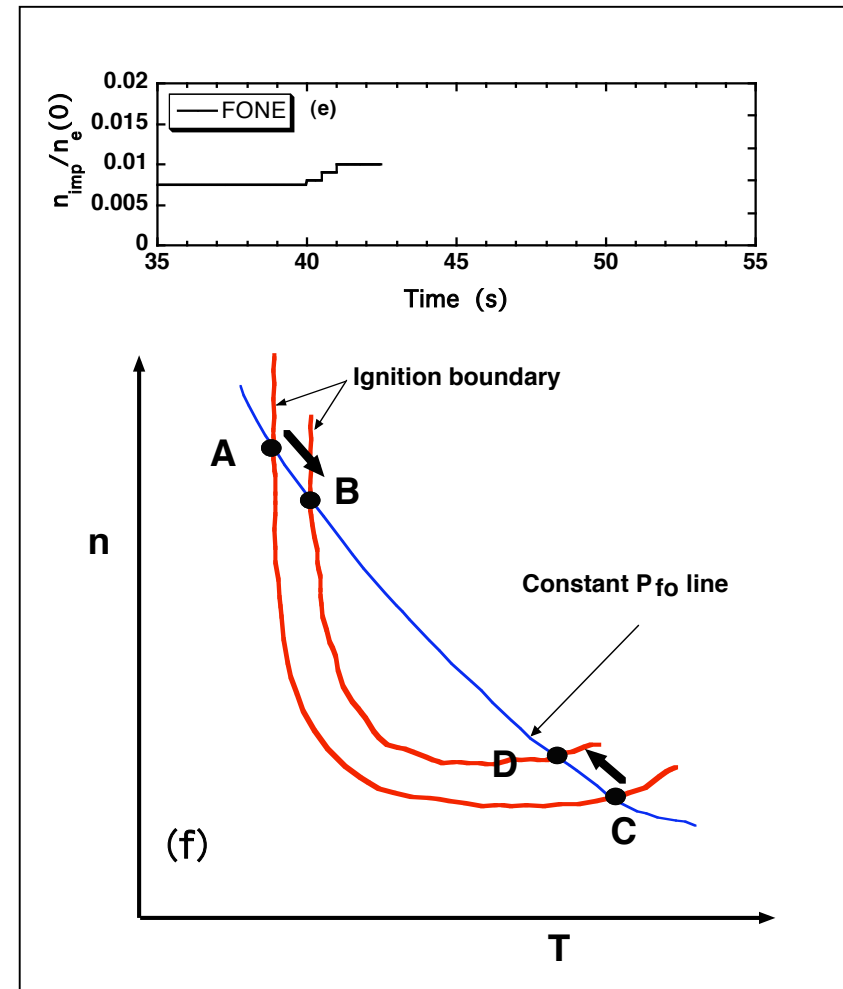
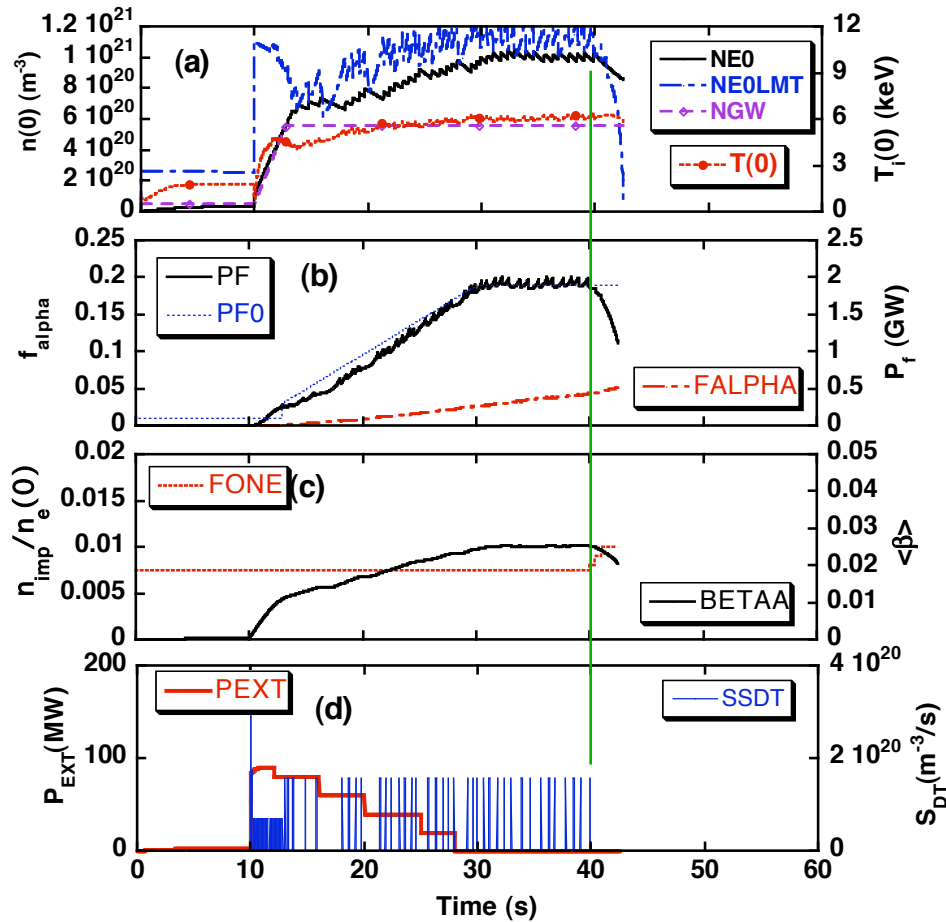
To ease pellet penetration, the temperature should be lowered.

He ash confinement time ratio should be lower as the confinement factor is reduced.

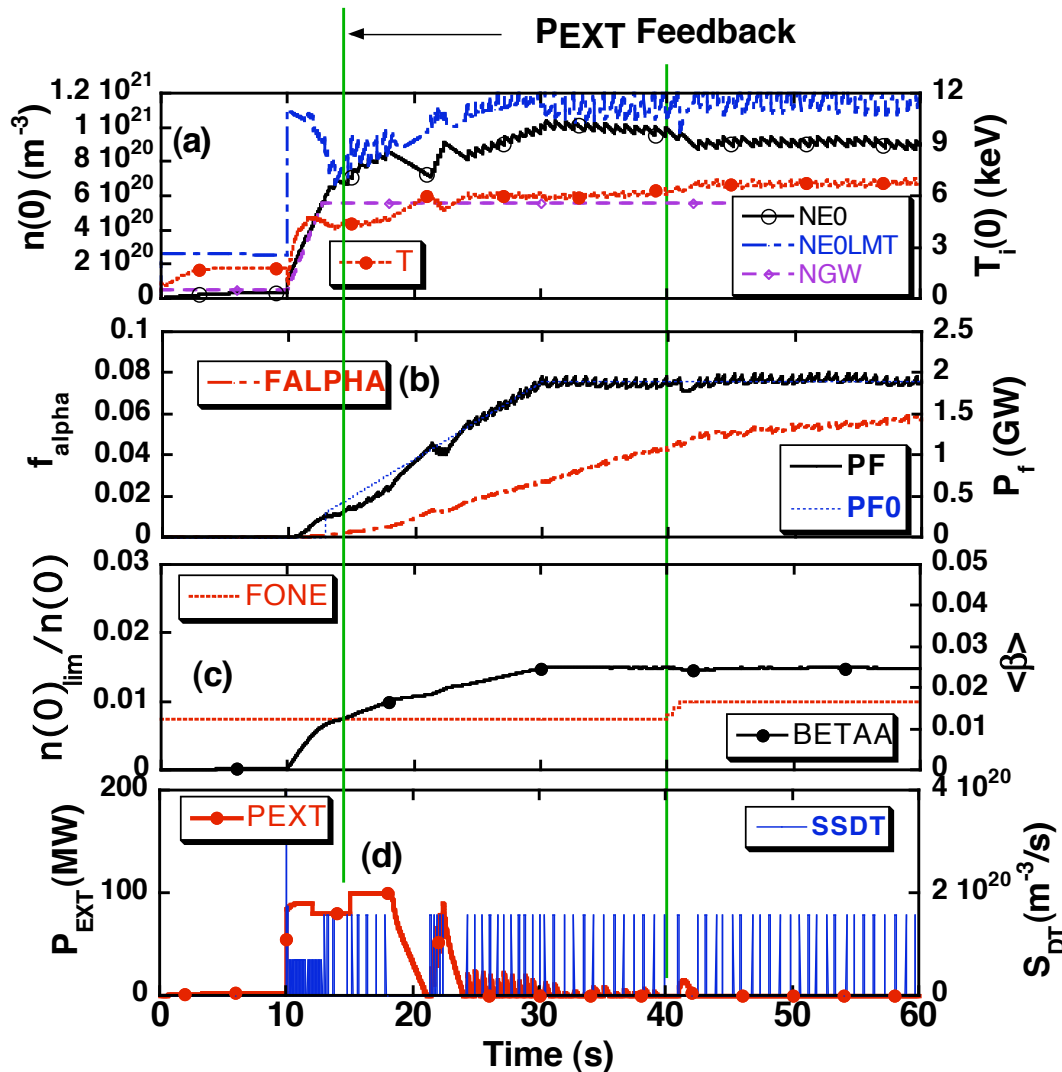
# 6. Control robustness to disturbances

## 6.1. Control of impurity disturbance by fueling alone: ( $\tau_p^*/\tau_E=3$ , $\tau_\alpha^*/\tau_E=3$ )

In general when the impurity fraction is increased, the density decreases, and temperature increases. **If it increases "quickly", ignition is terminated.**



## 6.1. Control of impurity disturbance by fueling and heating power: Feedback of heating power is switched on at 15 s. The heating power is automatically reduced, and becomes zero after oscillations, indicating ignition.



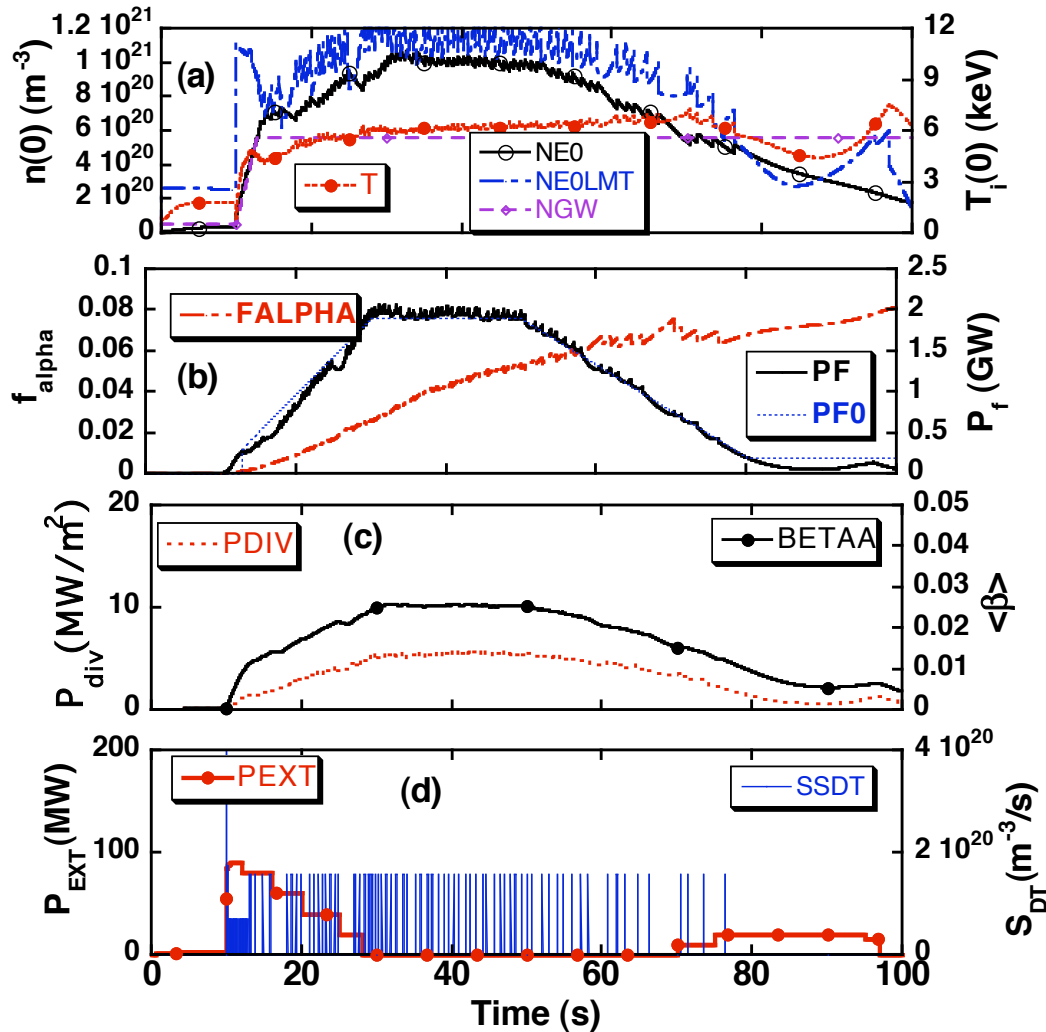
For the same increment of the impurity fraction, a small amount of heating power is applied by feedback, then ignition is recovered.

The temperature is increased and the density is decreased after impurity injection.

# 7. Shutdown phase

## 7.1. Shutdown phase-1

20 MW heating power provides the smooth fusion power shutdown.

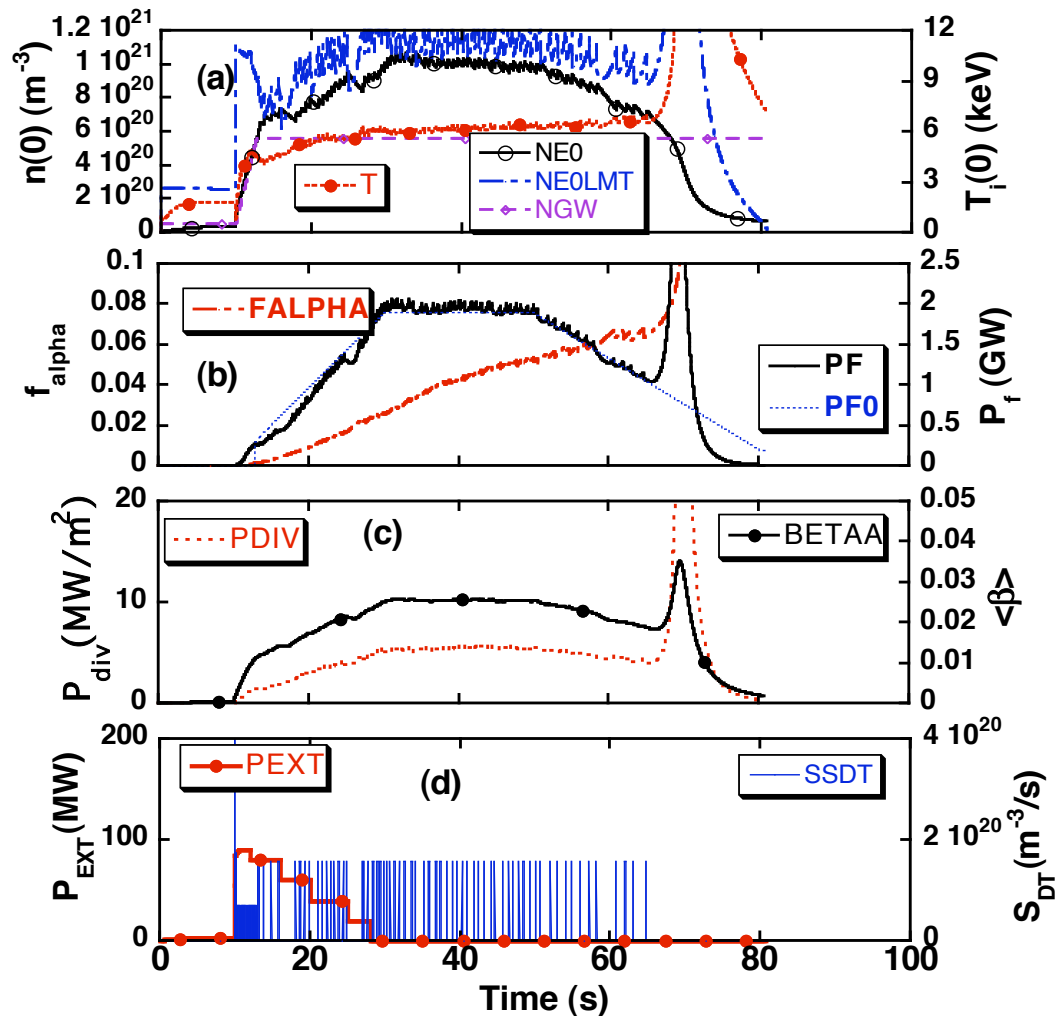


Without application of the heating power, the fusion power can be shutdown, but not smoother.



## 7.2. Shutdown phase-2

If fueling is stopped after 65s, excessive fusion power up to 4.25 GW is observed. Because, the thermal runaway takes place.



We always need the fueling control for unstable operation.

For forced shutdown, excessive fueling or killer pellet should be used.

## 8. Summary and further issues

- [1] It is possible to control the thermally unstable operating point even when the temperature and density change due to pellet injections.  
**Pellet size of 12 mm ~16 mm pellet are allowed for FFHR.**
- [2] To ease the pellet injection, the lower temperature ( $T(0) < 7$  keV) is desirable.  
**The conditions of  $\tau_{\alpha}^*/\tau_E < 4 \sim 5$  and  $\gamma_{ISS95} > 1.4$  are recommended in FFHR.**
- [3] Control robustness to impurity disturbances exists to some extent.  
**When feedback of the heating power is available, operational regime would be expanded.**
- [4] Shutdown of the unstable operation is no problem during the pellet injection.

### Further Issues

- [1] Unified control algorithm from ignition to sub-ignition.
- [2] Failure mode analysis should be conducted.
- [3] 1-D simulation should be done as soon as possible to take the profile effect into account during pellet injection for future application of this control method.